

Role of f-d exchange interaction and Kondo scattering in Nd doped pyrochlore Iridate $(\text{Eu}_{1-x}\text{Nd}_x)_2\text{Ir}_2\text{O}_7$

Sampad Mondal^{a,b,c*}, M. Modak^b, B. Maji^{b,d}, M. K. Ray^e, S.

Mandal^b, Swapan K. Mandal^a, M. Sardar^f and S. Banerjee^{b†}

^a Department of Physics, Visva-Bharati, Santiniketan 731235, India

^b Saha Institute of Nuclear Physics, HBNI, 1/AF Bidhannagar, Kolkata 700064, India

^c Ramsaday College, Amta, Howrah 711401, India

^d Acharya Jagadish Chandra Bose College, 1/1B, A. J. C. Bose Road, Kolkata 700020, India

^e Institute of Solid State Physics, University of Tokyo, Kashiwa 277-8581, Japan

^f Material Science Division, Indira Gandhi Centre for Atomic Research, Kalpakkam, India

We report study of magnetization, resistivity, magnetoresistance and specific heat of the pyrochlore Iridate $(\text{Eu}_{1-x}\text{Nd}_x)_2\text{Ir}_2\text{O}_7$ with $x=0.0, 0.5$ and 1.0 , where spin orbit coupling, electronic correlation, magnetic frustration and Kondo scattering coexists. Metal insulator transition temperature (T_{MI}) decrease with increase in Nd content but always coincides with magnetic irreversibility temperature (field induced moment). Resistivity below T_{MI} do not fit with either activated (gap) or to any power law (gapless) dependence. The Curie constant show surprising result, that Nd induces singlet correlation (reduction of para-moment) in Ir sublattice. Magnetoresistance is negative at low temperatures below 10 K and increases strongly with increase in x and vary quadratically with field switching over to linear dependence above 50 kOe. Low temperature specific heat shows Schottky peak, coming from Nd moments, showing existence of doublet split in Nd energy level, arising from f-d exchange interaction. All materials show presence of a linear specific heat in the insulating region. The coefficient of linear specific heat for $x = 0.0$ does not vary with external magnetic field but varies superlinearly for $x = 1.0$ materials. We argue that linear specific heat probably rules out weakly correlated phases like Weyl fermions. We propose that with the introduction of Nd at Eu site the system evolves from chiral spin liquid with gapless spinon excitations with a very small charge gap to Kondo type interaction superposed on chiral spin liquid coexisting with long range antiferromagnetic ordering. Huge increase of magnetoresistance with increase in Nd concentrations shows importance of Kondo scattering in the chiral spin liquid material by rare earth moments.

Introduction

Focus in condensed matter physics now a days is in understanding emergence of Dirac-like fermions under various circumstances.¹ A common theme is spin-orbit entanglement produced by spin-orbit interaction, influencing electronic and magnetic transitions.² Topology of the band structure is also important and it was suggested that in the weak correlation regime, quadratic band touching at some points in the Brillouin zone can lead to a large number of phases related to topological insulators, like three-dimensional Dirac³ and Weyl⁴ semimetals and axion insulator.⁵ Specifically in the magnetically ordered phase, where time reversible symmetry is broken but inversion symmetry is preserved, the pairs of quadratic band touching points lead to linearly dispersing Dirac fermion type spectrum, along with definite chirality, i.e. $\vec{k} \cdot \vec{\sigma} = \pm 1$, where \vec{k} and $\vec{\sigma}$ are unit vectors along the momentum and spin of electrons. This leads to many interesting properties like Hall effect without external magnetic field, negative/positive magnetoresistance when electric field and magnetic fields are parallel/perpendicular.⁶⁻⁸

In the strong correlation limit, the already narrow

bands due to spin-orbit coupling, may open up gap. With increase in local coulomb correlation, pairs of opposite chirality Weyl points move towards Brillouin zone boundary and annihilate pairwise to open up a gap, forming spin-orbit assisted Mott insulators.⁹ Owing to frustration in the magnetic exchange interaction (like in pyrochlores), one might get either metallic or insulating spin-liquid phases.¹⁰ This spin liquid phase, may also be chiral, but this time chirality is defined in terms of real space localised spin variables like $S_i \cdot S_j \times S_k$ developing non zero expectation values, where S_i, S_j, S_k are spins at sites i, j, k in a triangular plaquette. Interestingly this phase can also give anomalous Hall effect (without external magnetic field) and negative magnetoresistance like Weyl fermions if the transport gap is small.

To study the combined effect of spin-orbit coupling and electronic correlation, the $5d$ iridium oxides, like pyrochlore iridates $\text{Ln}_2\text{Ir}_2\text{O}_7$ where Ln is a lanthanide are the best candidates. The interpenetrating corner sharing tetrahedral structure is favourable to form a narrow flat band that enhances the effect of electron correlation and spin orbit coupling (SOC), and both of these energies are comparable to the band width. They also have a structure where antiferromagnetic interaction between magnetic ions is frustrated. These materials are proposed¹¹ to have many interesting topological phases and is being pursued by experimentalists to discover interesting properties of matter.

*Email:sampad100@gmail.com

†Email:sangam.banerjee@saha.ac.in

$\text{Ln}_2\text{Ir}_2\text{O}_7$ (R=rare earth) have shown many interesting transport and magnetic properties,¹²⁻¹⁴ and shows a transition from incoherent and strongly correlated metal (at high temperature) to an antiferromagnetically ordered insulator/semimetal (at low temperature) except when $\text{Ln}=\text{Pr}$. Transition temperature decreases as the ionic radius of the rare earth atom increases.¹⁴ Metal to insulator/semimetal transition is reminiscent of Mott-Hubbard transition but with the added complexity, that (1) spin and orbital degrees of freedoms are entangled due to spin-orbit coupling, (2) both transition metal and rare earth sublattices are magnetically frustrated, and (3) there is local Kondo coupling (f-d exchange interaction) between localised rare earth moments and the transition metal electrons. In $\text{Eu}_2\text{Ir}_2\text{O}_7$ we can avoid f-d exchange interaction because net moment of Eu^{3+} is zero. This is a suitable system to study the effect of both SOC and electronic correlation. A continuous phase transition from paramagnetic metal to antiferromagnetic insulating state was observed in single crystals.¹⁵ Low frequency optical conductivity¹⁶ increases linearly with frequency. This is consistent with a Dirac-like spectrum with density of states varying linearly with energy, suggesting that $\text{Eu}_2\text{Ir}_2\text{O}_7$ is a Weyl Semimetal. From analysis of resistivity, Tafti et al.¹⁷ have suggested that $\text{Eu}_2\text{Ir}_2\text{O}_7$ goes from paramagnetic metal to Weyl semimetal (in an intermediate temperature window) and finally to an antiferromagnetic insulator at the lowest temperature. Paradoxically in the low temperature region (below 10 K) the optical conductivity was also found to be proportional to frequency. When the rare earth sites have moment (like Nd) the f-d exchange interaction (Kondo) can mediate RKKY type exchange interaction between the localized rare earth moments, which along with superexchange interaction between themselves, may induce the ordering of Nd sub lattice system. The magnetic ordering of Nd sub system can in turn modify the electronic structure of the Ir sub system, promoting many exotic quantum correlated phenomena. Even when Nd moments are not ordered yet, the Kondo scattering between f and d electrons can profoundly affect the electronic properties of Ir electrons. Weyl fermion is a weak correlation concept and are unlikely to survive with increase in correlation. It has been argued¹⁸ that f-d interaction along with strong correlation can again stabilize Weyl Semimetal phase. Polycrystalline $\text{Nd}_2\text{Ir}_2\text{O}_7$ shows metal insulator transition at 33 K.¹⁹ Raman scattering confirms that there is no structural change accompanying metal insulator transition.²⁰ Optical,²¹ transport²² and photoemission²³ experiments suggest a gapped insulating ground state in $\text{Nd}_2\text{Ir}_2\text{O}_7$. $\text{Nd}_2\text{Ir}_2\text{O}_7$ compound develops a long range antiferromagnetic all-in-all-out (AIAO) ordering of the Nd moments²⁴ below 15 K (though the magnitude of ordered Nd moments is very small), confirmed by inelastic neutron scattering measurement.²⁵ Long range antiferromagnetic ordering is destroyed by applied magnetic field, producing a field induced insulator to metal transition.^{22,26} We have prepared polycrystalline $\text{Eu}_{2(1-x)}\text{Nd}_x\text{Ir}_2\text{O}_7$ with $x=0.0$,

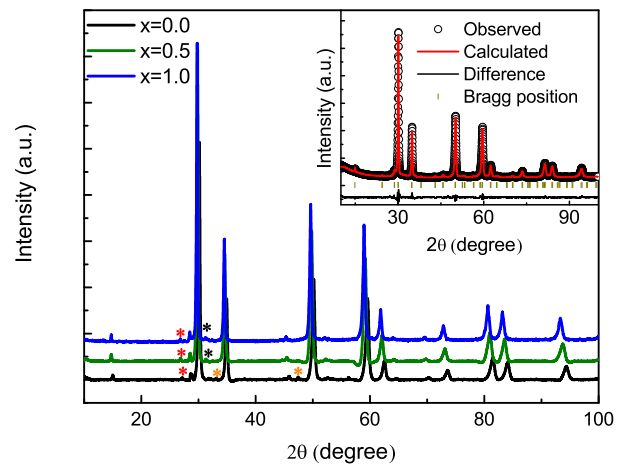


FIG. 1: Room temperature X-ray diffraction pattern for the sample $(\text{Eu}_{1-x}\text{Nd}_x)_2\text{Ir}_2\text{O}_7$ where $x=0, 0.5, 1.0$ and red, orange and black stars are indicating the impurity phase due to non-reacting IrO_2 , Eu_2O_3 and Nd_2O_3 respectively. Inset fig. shows Rietveld refinement for $x=0.0$ compound, where scattered data are observed and solid line is fit to the data.

0.5 and 1.0, and have studied resistivity, magnetoresistance, magnetization and specific heat with and without magnetic field.

Experimental details

All the polycrystalline samples were prepared by solid state reaction method. High purity ingredient powder Eu_2O_3 , IrO_2 and Nd_2O_3 were mixed in stoichiometric ratio and ground well. After pressing the mixture powder in pellet form, heated at 1373 K for 3 days with several intermediate grinding. All the samples were characterised by powder X-ray diffraction (XRD). The room temperature XRD measurement was taken by X-ray diffractometer with $\text{Cu K}\alpha$ radiation. Structural parameter were determined using standard Rietveld technique with Fullprof software package. Magnetic measurement was taken by Superconducting Quantum Interference Device Magnetometer (SQUID-VSM) of Quantum Design in the temperature range 3 K - 300 K. Electrical, magnetic and thermal transport measurements were carried out by Physical Properties Measurement System (PPMS).

Experimental results

Room temperature XRD pattern for the samples $(\text{Eu}_{1-x}\text{Nd}_x)_2\text{Ir}_2\text{O}_7$ with $x=0.0, 0.5, 1.0$ are shown in fig. 1. There is no modification of the XRD pattern but peaks shift to lower angles with Nd substitution at Eu site. Observed data of all samples are refined on the basis of cubic structure with space group Fd-3m by Rietveld refinement method. Refinement of the $x=0.0$ compound is shown in the inset of fig. 1. All the samples are nearly in pure phase except some minor impurity phases (non-reacting oxide) which are marked by star. In $x=0.0$ com-

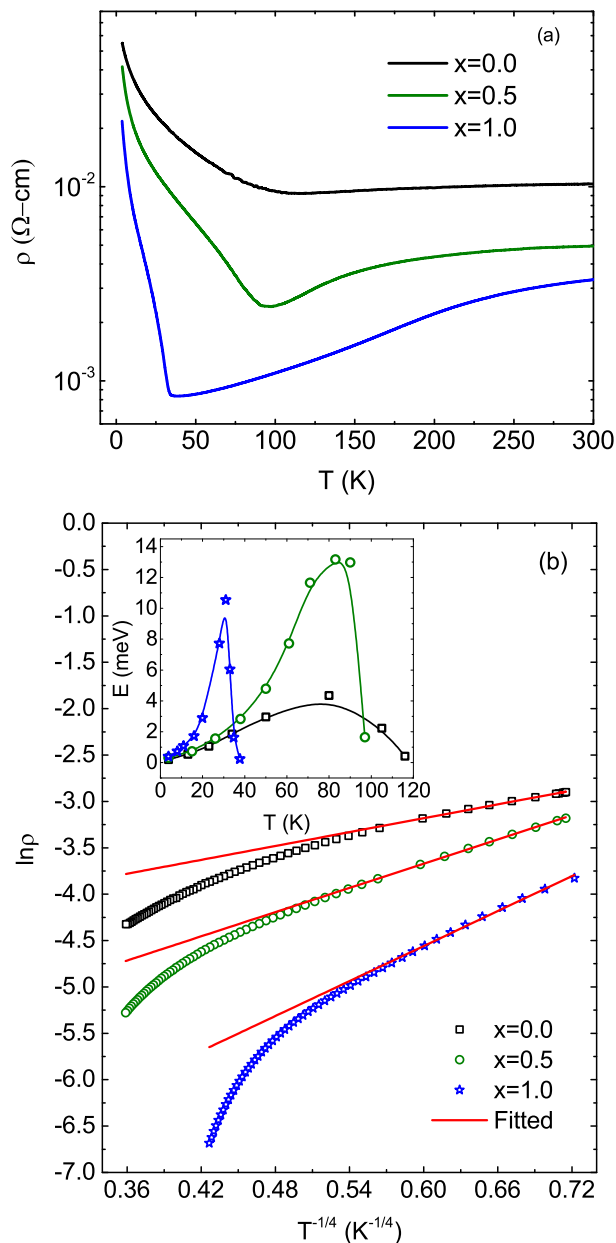


FIG. 2: (a) Temperature dependent resistivity measured with temperature range 3.8-300 K and (b) Fitting of resistivity below MIT for the compounds $(\text{Eu}_{1-x}\text{Nd}_x)_2\text{Ir}_2\text{O}_7$ where $x=0, 0.5$ and 1.0 and inset shows variation of charge gap (E) with temperature for all the samples.

compound, impurity phases due to non-reacting oxide IrO_2 and Eu_2O_3 are 0.62% and 0.89% respectively and IrO_2 , Nd_2O_3 impurity phases in $x=0.5$ and 1.0 compounds are 0.72%, 0.69% and 0.78%, 0.82% respectively. Obtained lattice parameters from Rietveld refinement for $x=0, 0.5$ and 1.0 compounds are 10.3142 \AA , 10.3472 \AA and 10.3858 \AA respectively. The increase of lattice parameter with Nd doping indicates that Eu^{3+} is substituted by larger ionic radius Nd^{3+} .

Fig. 2(a) shows temperature dependent resistivity of the sample $(\text{Eu}_{1-x}\text{Nd}_x)_2\text{Ir}_2\text{O}_7$ with $x=0, 0.5$ and 1.0 from 3 K to 300 K. All samples show metal to insulator transition (MIT) i.e. $\frac{d\rho}{dT}$ changes from positive to negative below the MIT temperature (T_{MI}). Observed MIT temperatures of $x=0, 0.5$ and 1.0 compounds are 120 K, 95 K and 35 K respectively. Both T_{MI} as well as the resistivity in the entire temperature range decreases with Nd doping. This is consistent with earlier observations¹⁴ that T_{MI} decreases with increase in rare earth ionic size. From Rietveld refinement we find higher ionic radii ion Nd doped at Eu site increases the bond angle between Ir-O-Ir which increases the Ir-O orbital overlap leading to increase Ir-Ir hopping matrix element, i.e. Ir t_{2g} band width.²⁷ The MI transition gives the appearance of a straightforward Mott-Hubbard transition (competition between hopping matrix element and Local Hubbard repulsion), but attempt to fit the resistivity in the insulating phase with activated form (with a gap) fails, as it shows that the gap is temperature dependent with a maximum below T_{MI} and very small near 3 K and T_{MI} (see inset fig. 2(b)). On the other hand μSR experiments in Eu and Nd compounds show continuous rise of well defined muon precession frequency below T_{MI} ,^{28,29} indicating long range magnetic ordering into a commensurate structure, as is expected in an antiferromagnetically ordered Mott insulating state. Antiferromagnetic ordering can emerge in weak coupling (small Hubbard U) theories like in Slater antiferromagnetic state also but the temperature dependence of transport gap is disturbing. It has been suggested theoretically³⁰ that arbitrarily small antiferromagnetic ordering of Ir electrons can convert quadratic band touching points into a Weyl semimetal phase with Dirac cone linear dispersions at some points on the Brillouin zone. Optical conductivity in $\text{Eu}_2\text{Ir}_2\text{O}_7$ measured at 7 K shows¹⁶ a linear dependence on frequency at the lowest frequencies, consistent with density of states $\rho(E) \propto |E - E_F|$ expected out of a Weyl semimetal. This should also mean that the low temperature resistivity must vary with temperature as $\frac{1}{T}$ and was predicted theoretically.¹ We find that resistivity of none of the samples varies in a power law ($\frac{1}{T^\alpha}$) fashion from 3 K to T_{MI} . Single crystal resistivity measurement¹⁵ of $x=0.0$ showed a surprising result i.e., the temperature dependence of resistivity of all single crystals (made in the same batch) coincides above T_{MI} , while below T_{MI} there is wide discrepancies in resistivity values between samples, and the residual resistivity at the lowest temperature varies by two orders of magnitude between samples. There are two sources of possible disorder, (1) slight difference in oxygen concentration¹⁵ and (2) interchange of a small fraction of Eu and Ir sites.³¹ Both has the net effect of doping hole in the half filled Ir sub system. It is found that more stoichiometric materials have larger residual resistivity.¹⁵ Sr doping in $\text{Eu}_2\text{Ir}_2\text{O}_7$ ³² and Ca doping in $\text{Nd}_2\text{Ir}_2\text{O}_7$ ³³ leads to reduction of T_{MI} and both systems above T_{MI} shows non fermi liquid properties. More importantly it is found³⁴ that $\text{Nd}_2\text{Ir}_2\text{O}_7$

TABLE I: Fitting parameter T_0 and temperature range obtained from VRH model for the sample $(\text{Eu}_{1-x}\text{Nd}_x)_2\text{Ir}_2\text{O}_7$

Sample	Temperature range (K)	$T_0(\text{K})(10^3)$
x=0.0	3.8-14	0.038
x=0.5	3.8-19	0.357
x=1.0	3.8-12	1.559

fragments into magnetic domains separated by domain walls, and the domain wall region has much lower resistivity than within the magnetic domains, i.e. the measured conductivity is that of the domain walls and not of bulk. Assuming the antiferromagnetic regions as topological insulators, the domain walls might have gapless surface states. It is to be noted that topological insulator and Weyl metal/semimetals arise due to chirality in momentum space. Moreover optical²¹ and transport²² and photoemission²³ experiments suggest a gapped insulating ground state in $\text{Nd}_2\text{Ir}_2\text{O}_7$. In view of the fact that there is unavoidable non-stoichiometry as well as domain formation in these materials, it is worthwhile to look at theoretical³⁵ analysis of disordered Weyl metals. Main conclusions from theoretical calculations are, (1) resistivity crosses over to $\frac{1}{T^{0.5}}$ from $\frac{1}{T}$ (for clean Weyl metal), and (2) the magnetoresistance at low field is positive (anti-localisation, because of spin orbit coupling) and switches over to negative at higher field. Both of these are not observed in our materials.

On the other hand we find that resistivity of all three samples can be fitted to, 3-dimensional Mott variable range hopping (VRH) model³⁶

$$\rho = \rho_0 \exp((T_0/T)^{1/4}) \quad (1)$$

where, $T_0 = \frac{21.2}{N(E_F)\xi^3}$, $N(E_F)$ and ξ are density of states at Fermi level and localization length respectively. It fits data well but only within a limited range of temperature (less than one order of magnitude i.e., from 3 K to 20 K only). T_0 increases with Nd doping. Assuming that density of states does not vary much between the samples, it shows that ξ decreases with increase in Nd concentration, but since the fit is over such a small range of temperatures, we do not force this point (strong localization).

Fig. 3(a-c) shows temperature dependent susceptibility of the samples in zero field cooled (ZFC) and field cooled (FC) protocol, measured under applied magnetic field of 1 kOe within temperature range 3 K - 300 K. M_{ZFC} for parent compound increases with decrease in temperature with a weak magnetic anomaly close to 120 K. M_{FC} merges with M_{ZFC} up to temperature 120 K, below which there is a bifurcation between M_{ZFC} and M_{FC} . The magnetic irreversibility start at $T_{irr} \approx 120$ K. RXD (Resonant X-ray diffraction) and μSR (Muon spin rotation and relaxation) measurements have shown that below T_{irr} , Ir moments order antiferromagnetically (all-

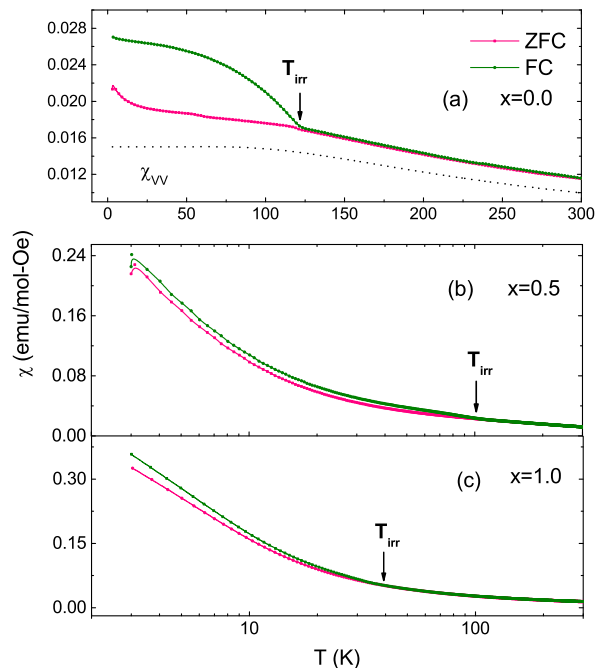


FIG. 3: (a-c) Temperature dependent magnetization measured at 1 kOe in ZFC FC protocol for $(\text{Eu}_{1-x}\text{Nd}_x)_2\text{Ir}_2\text{O}_7$ where $x=0, 0.5, 1.0$ and dotted line for $x=0$ compound represents van vleck susceptibility χ_{VV} of Eu^{3+} ion.

TABLE II: θ_p, μ_{eff} for $(\text{Eu}_{1-x}\text{Nd}_x)_2\text{Ir}_2\text{O}_7$ system.

Sample	θ_p (K)	μ_{eff} ($\mu_B/\text{f.u.}$)
x=0.0	-175	2.40
x=0.5	-127	6.41
x=1.0	-175	7.35

in/all-out or AIAO),^{28,37} though it needs emphasis that magnitude of ordered moment is very small. As the interval energy level of Eu^{3+} and Sm^{3+} , between the ground state and the successive first excited state is comparable with the thermal energy at the room temperature, they shows temperature dependent Van Vleck susceptibility.³⁸ To obtain the contribution of Ir moment in parent compound, we subtracted Van Vleck susceptibility χ_{VV} due to Eu^{3+} ion from χ . Temperature dependent χ_{VV} was calculated by using $\lambda = 400$ K,³⁸ and is shown in fig. 3(a) by dotted line. Doped sample also shows bifurcation but lesser in magnitude compared to parent compound. T_{irr} decreases with Nd concentration. T_{irr} for $x=0, 0.5$ and 1.0 samples are 120 K, 100 K and 38 K respectively and are identical with T_{MI} . No magnetic anomaly of M_{ZFC} is seen in doped samples down to the lowest temperature.

Fig. 4(a-c) shows temperature dependent inverse susceptibility in the entire temperature region, fitted in the temperature range 140-290 K with Curie-Weiss law $\chi = \frac{C}{T-\theta_p}$, θ_p is Curie Weiss temperature, and Curie

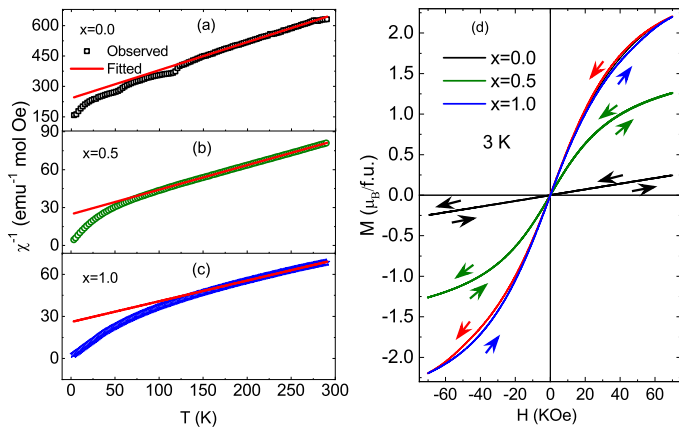


FIG. 4: (a-c) Temperature dependent inverse susceptibility and (d) Isothermal magnetization at 3 K for $(\text{Eu}_{1-x}\text{Nd}_x)_2\text{Ir}_2\text{O}_7$ where $x=0, 0.5$ and 1.0 .

constant $C = \frac{N_A \mu_{eff}^2}{3K_B}$, and μ_{eff} is the effective paramagnetic moment. θ_p , μ_{eff} for all the samples are shown in table II. At the high temperature region (140-290 K) all the materials show Curie-Weiss susceptibility. As the temperature decreases inverse susceptibility deviates from linear dependence with changing its slope below 140 K. At very low temperatures, inverse susceptibility starts bending down towards low values, presumably because of pure Curie contribution coming from some noninteracting isolated moments. All the sample shows negative θ_p at the high temperature region, indicates antiferromagnetic interaction. It is hard to determine the exact moment contribution of Nd^{3+} and Ir^{4+} from this measurement. If we assume the contribution of magnetic moment for Nd^{3+} ($3.57 \mu_B$) from reported $\text{Nd}_2\text{Sn}_2\text{O}_7$ ³⁹ where Sn^{4+} has no moment, then the contribution of Ir local moment in the metallic phase for $x=0.5$ and 1.0 compounds are $1.42 \mu_B$ and $0.11 \mu_B$ respectively. This indicates that Ir moment decreases with Nd doping. Decrease of Ir para-moment in doped materials indicates occurring of strong singlet correlation between Ir moments by f-d exchange interaction with Nd moments.

Isothermal magnetization data (M-H) taken at 3 K, up to magnetic field 70 kOe of all samples are shown in fig. 4(d). Parent compound shows linear behavior without any magnetic saturation up to magnetic field 70 kOe. $x=0.5$ and 1.0 compounds show non-linear behavior without any magnetic saturation up to field 70 kOe. Magnetic moment increases with Nd doping and moment at 70 kOe, of $x=0.0, 0.5$ and 1.0 compounds are $0.246 \mu_B/\text{f.u.}$, $1.263 \mu_B/\text{f.u.}$ and $2.20 \mu_B/\text{f.u.}$ respectively. This low value compared to paramagnetic moments given in table II clearly indicates onset of antiferromagnetic ordering. Close view of fig. 4(d) shows that coercive field (H_C) and remanent magnetization (M_r) for $x=0.0$ and 0.5 and 1.0 compounds are 0.0 Oe, 30 Oe, 20 Oe and 0.0 , 4.16×10^{-5} and $8.29 \times 10^{-4} \mu_B/\text{f.u.}$ respectively.

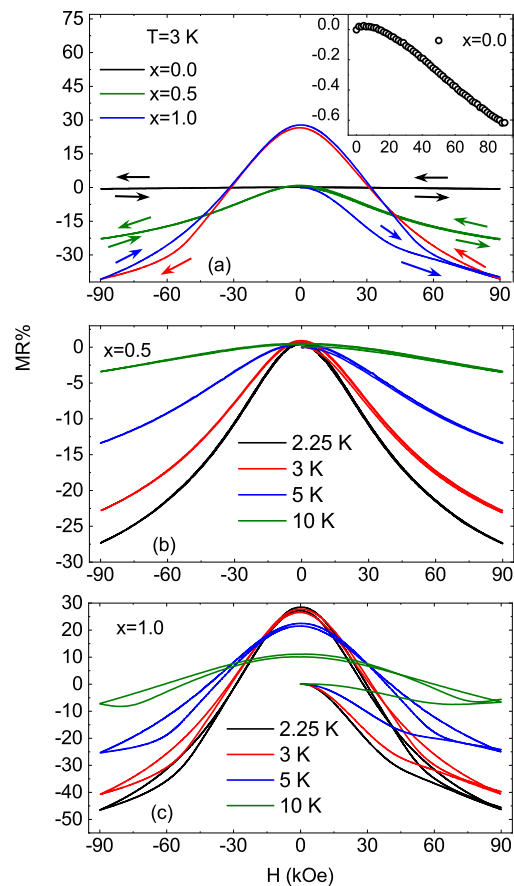


FIG. 5: (a) Magnetic field dependent MR for $(\text{Eu}_{1-x}\text{Nd}_x)_2\text{Ir}_2\text{O}_7$ where $x=0, 0.5$ and 1.0 , at 3 K with field -90 kOe to +90 kOe and inset shows close view field dependent MR for $x = 0.0$ (b, c) Magnetic field dependent MR for $x=0.5$ and 1.0 compounds at different temperatures.

Magnetoresistance (MR) defined by $[\rho_H - \rho_0]/\rho_0$, where ρ_0 and ρ_H are resistivity without and with applied field are shown in fig. 5(a-c). Fig. 5(a) shows magnetic field dependent MR at 3 K for all the samples. The parent compound shows very small negative MR (0.6 % at 90 kOe), which varies quadratically at low field (see inset fig. 5(a)) and switch to linear field dependency beyond 50 kOe, though Mathshira et al.¹⁹ reports small and positive magnetoresistance at all temperatures. $x=0.5$ and 1.0 material show large negative magnetoresistance, varying quadratically at low fields and switching over to linear dependence beyond 50 kOe. Magnitude of negative magnetoresistance keep increasing with decrease in temperature and at 2.25 K and 90 kOe, reaches 28 % and 45 % in $x=0.5$ and 1.0 compounds respectively, shown in fig. 5(b-c). $x=1.0$ compound shows a hysteresis loop between 1st up and down sweep of the field. This hysteresis loop in MR for $x=1.0$ is also accompanied by tiny hysteresis in isothermal magnetization data. It is clear that negative magnetoresistance increases dramatically only with incorporation of Nd moment and its interaction (f-d exchange) with Ir electrons. Another feature

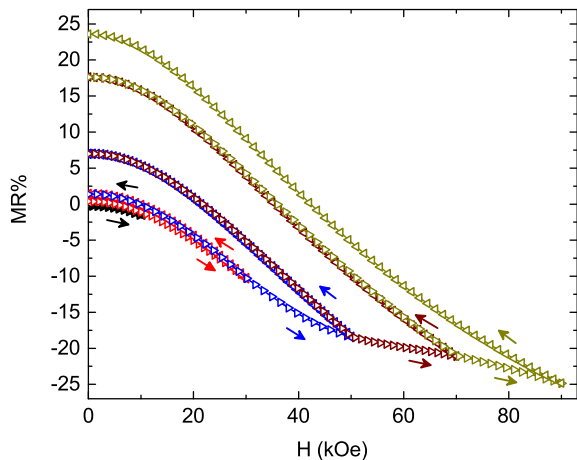


FIG. 6: Different magnetic field cycling MR at 5 K for the compound $(\text{Eu}_{1-x}\text{Nd}_x)_2\text{Ir}_2\text{O}_7$ where $x=1.0$.

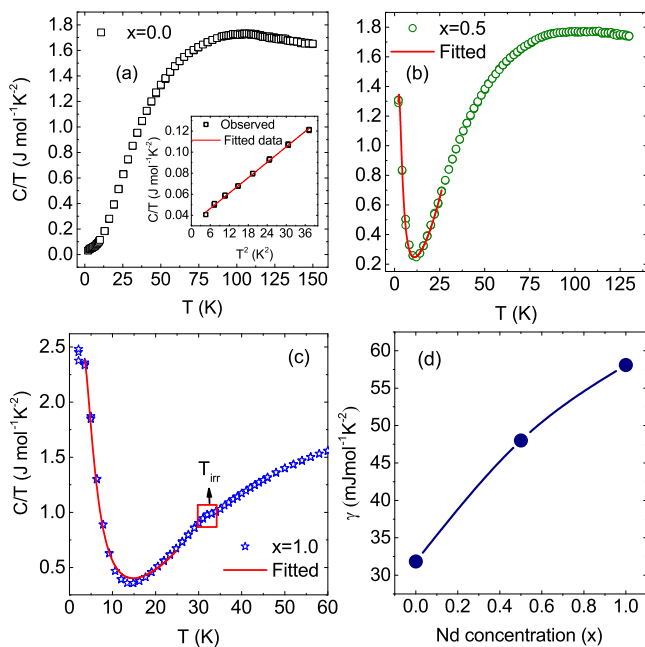


FIG. 7: (a-c) Zero field specific heat (C/T) as a function of temperature between different temperature range for $x=0.0$, 0.5 and 1.0 compound respectively and solid lines are fitting data. Inset of fig. 7 (a) shows C/T vs. T^2 data at low temperature for $x=0.0$ compound. (d) Variation of γ with Nd doping.

i.e., increase of resistance when the magnetic field is cycled back to zero field, as shown in fig. 6, is proportional to the magnitude of magnetic field cycle. This has been explained in the discussion section.

Fig. 7(a-c) shows temperature variation of heat capacity in the temperature range 2.1-150 K, 2.1-130 K and 2.1-60 K for $x=0.0$, 0.5 and 1.0 compounds respectively during warming. We observe that there is no anomaly at

the T_{irr} for $x=0.0$ and 0.5 compound though for $x=1.0$ compound shows a faint anomaly at 35 K. Inset in fig. 7(a) shows C/T vs. T^2 data for $x=0.0$ compound. We get excellent fit to specific heat within the temperature region 2.1-6 K, by assuming,

$$C = \gamma T + \beta T^3 \quad (2)$$

The fitting parameters γ and β are $31.8 \text{ mJ mol}^{-1} \text{ K}^{-2}$ and $0.954 \text{ mJ mol}^{-1} \text{ K}^{-4}$. The γ value is close to $33 \text{ mJ mol}^{-1} \text{ K}^{-2}$ reported by Ishikawa et al.¹⁵ It is important to point out that a linear in temperature term is absolutely necessary to fit the data at lower temperatures ($T < 30 \text{ K}$). This is surprising because in that temperature region the resistivity is non metallic. Weakly localized Fermi liquids can give linear specific heat, because of finite density of states near Fermi energy, but the resistivity of parent compound does not follow $\frac{1}{T^{0.5}}$ for a 3-dimensional dirty metal. In strongly localized Fermi systems (that shows variable range hopping type of conductivity), specific heat comes purely from spin degrees of freedom and is not linear. Moreover in strong localization limit spin susceptibility does not follow Curie Weiss form as we observe. Dirac or Weyl fermions with linear energy dispersion gives a T^3 specific heat. Spin waves (bosons) about antiferromagnetically ordered state also don't give linear specific heat. We shall comment on it in discussion section.

In fig. 7(b-c) we see anomalous increase of specific heat at low temperatures, in both $x=0.5$ and 1.0 compounds, that looks like a Schottky type anomaly. We get good fit by assuming,⁴⁰

$$C = \gamma T + \beta T^3 + n \left(\frac{\Delta_0}{T}\right)^2 \frac{\exp(\Delta_0/T)}{(1 + \exp(\Delta_0/T))^2} \quad (3)$$

where n and Δ_0 are proportional to the number of two level systems and the energy separation between two levels respectively.

The fitting parameters γ , β , n and Δ_0 for $x=0.5$ and 1.0 compounds are $48 \text{ mJ mol}^{-1} \text{ K}^{-2}$, $0.945 \text{ mJ mol}^{-1} \text{ K}^{-4}$, 8.2 , 7.83 K (0.67 meV) and $58.1 \text{ mJ mol}^{-1} \text{ K}^{-2}$, $0.907 \text{ mJ mol}^{-1} \text{ K}^{-4}$, 19.82 and 10.35 K (0.89 meV) respectively. We note that the value of Δ_0 is very similar to the reported value obtained using inelastic neutron scattering (i.e., 1.3 meV).^{25,41} Coefficient γ increases with Nd doping, but β does not vary much. Both the number of degrees of freedom n and energy separation between two level Δ_0 increases with Nd doping. We suggest that, Schottky anomaly occur because of an effective molecular field H_{mf} via f-d exchange interaction present at the Nd sites once the weak AIAO antiferromagnetic transition of Ir moments sets in as suggested earlier for this system.^{25,41} Nd^{3+} is Krammer ion, and H_{mf} splits the ground state doublet of each Nd^{3+} at low temperature. If the effective moment of Nd^{3+} is μ_{Nd} then $\Delta_0 = 2\mu_{Nd} H_{mf}$. There will be some additional contribution to H_{mf} from Nd-Nd superexchange interaction in a mean field sense.

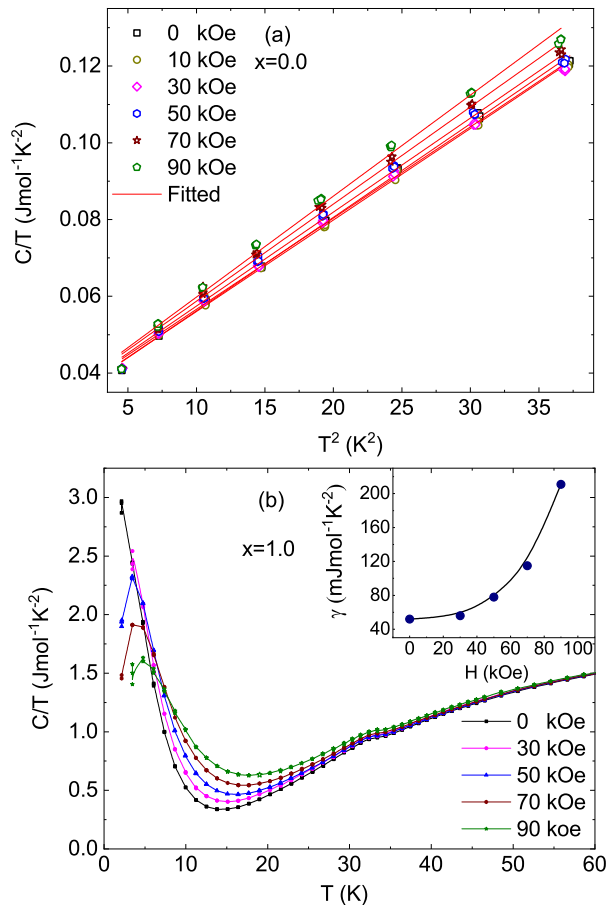


FIG. 8: (a) C/T vs. T^2 data with different field for $x=0.0$ compound with fitting. (b) Magnetic field dependent specific heat as a function of temperature for $x=1.0$ compound. Inset shows field dependent γ .

Fig. 8(b) shows that the peak (Schottky) temperature progressively shifts towards higher temperature (i.e., Δ_0 increases with applied magnetic field) and the peak height decreases due to increase in ordering (decrease in entropy) as we increase the external magnetic field from 0.0 to 90 kOe. This is typical of Schottky peak coming from localised two level systems of spin origin (Nd moment).

More interesting is the magnetic field dependence of linear specific heat coefficient γ for $x=1.0$. Fig. 8(a) shows that in $x=0.0$ material γ does not vary with magnetic field as was observed earlier in spin 1/2 gapless spin liquid.^{42,43} In $x=1.0$ material on the other hand γ varies superlinearly with magnetic field beyond 30 kOe and shows no sign of saturation even at 90 kOe (see inset in fig. 8(b)). Both linear specific heat and its curious variation with magnetic field was not seen before in pyrochlore iridate compounds, and in discussion section we point out the possible origin.

Discussion

Physics of pyrochlore iridates is dictated by 5d electrons of Ir, which has strong spin-orbit coupling and a moderate Hubbard repulsion U (due to large spatial extent of 5d orbitals). Combined effect of octahedral crystal field of oxygen anions and spin-orbit coupling leads to an effective single band (half filled) description in terms of pseudo spin (spin-orbit entangled) $J_{eff} = 1/2$ states.

Resistivity, as we have already discussed has two main problems, (1) inherent disorder due to interchange of rare earth and transition metal sites, and any other off-stoichiometry due to oxygen concentration and (2) The observation of domain formation and lower resistance in domain boundary region than in the bulk. Therefore transport measurements do not reflect precise electronic states in the bulk.

Both Ir and Nd ion sublattices are pyrochlore lattice. Superexchange interaction between Ir-Ir and Nd-Nd moments are antiferromagnetic. Moreover due to spin-orbit coupling both Ir and Nd pseudo spin 1/2's have single ion anisotropy along local [111] axis (towards the center of tetrahedras). The ground state of such a model is AIAO ordering for both Ir and Nd moments. The f-d exchange interaction has been derived theoretically.¹⁸ It is seen that f-d interaction is such that, a local AIAO ordering of Ir moment, gives an effective magnetic field at Nd moments sites encouraging AOAI ordering of Nd moments. Reason for magnetic irreversibility (field induced moment) is puzzling. It is true that magnetic field can destabilise AIAO ordering and lead to 3-in-1-out or 2-in-2-out states, because their energies might be very close to AIAO magnetic state. All these states have a net moment per tetrahedra (unlike in AIAO state), but these net moment must alternate going from one tetrahedra to the next, and an increase in magnetization induced by magnetic field is not expected. We suggest that induced moment comes because of inherent disorder of the kind we mentioned before. Suppose a few Ir and Eu ions switch sites (interchange) in $\text{Eu}_2\text{Ir}_2\text{O}_7$. Then If an Eu^{3+} ion (zero net pseudospin) sits at an Ir site, then Ir moments in all tetrahedras connected to this site will deviate from AIAO ordering, i.e. those tetrahedras will pick up a net magnetic moment. Secondly Ir electron from a near neighbour site can now hop into empty 5d orbital of Eu or Nd ions (delocalisation of Ir electrons through Eu/Nd on Ir sublattice sites), creating an effective double exchange type local ferro correlation along with a net moment.

As the material cools down from high temperature, slowly Ir-Ir superexchange and magnetic anisotropy takes over and Ir moments starts ordering (AIAO) below $T=120$ K, though the observed magnitude of AIAO ordered Ir moments are very small.²⁵ The AIAO ordering of Ir moments gives an effective magnetic field at Nd moment sites. This is visible from the observed Schottky peak in the specific heat data for $x=0.5$ and 1.0 compound. However, the inverse susceptibility tending towards zero value in fig. 4(a-c) indicates a paramagnetic background at low temperature.

It has been argued⁴⁴ that real space spin chirality,

defined as $\chi_{ijk} = S_i \cdot S_j \times S_k$ is responsible for negative magnetoresistance. Spin chirality⁴⁵ can be written in terms of underlying electron operators (fermions) as, $\frac{i}{2}\chi_{ijk} = P_{ijk} - P_{ikj}$, where $P_{ijk} = \chi_{ij}\chi_{jk}\chi_{ki}$ and $\chi_{ij} = C_{i\sigma}^\dagger C_{j\sigma}$, where C 's are electron operators. A non zero value of χ_{ijk} leads to a Berry phase picked up by electrons as it circulates around a triangular plaquette, i.e as if spin chirality creates a fictitious magnetic field perpendicular to the plaquette. This chirality has to be contrasted with chirality of Weyl fermions near Weyl points, that are created by a singular Berry phase in momentum space.⁴⁶ This kind of real space spin chirality can give Hall effect without magnetic field as observed in MnSi⁴⁷ and negative magnetoresistance.⁴⁸ When spin chirality of all triangular plaquettes are staggered or along random direction, the magnetoresistance varies quadratically with magnetic field. At higher magnetic field when the chirality of most triangular plaquettes are preferably aligned along some direction then asymmetric scattering of electrons by spin chirality can occur and one gets odd-parity magnetoresistance, i.e magnetoresistance varying linearly with magnetic field. Therefore the magnetic ordering of Ir electrons can be thought of as a weak antiferromagnetic (AIAO) long range ordering (Reported earlier by RXD and μ SR measurement^{28,37}) superimposed on a chiral spin liquid state.^{8,49-51}

Huge increase in magnetoresistance with increase in Nd, points out importance of Nd moments. We suggest that, apart from the scattering of carriers in the domain walls by chirality fluctuations, there is an additional Kondo scattering of carriers by Nd electron moments. Kondo scattering in heavy fermion materials give quadratic field dependent at low field and linear at high field negative magnetoresistance.⁵² For Nd doping the resistance value increases after a field cycle is due to reduction of domain wall i.e., in between either AIAO-AOAI or vice versa ordered regions.³⁴ This was noticed before in $\text{Pr}_2\text{Ir}_2\text{O}_7$ ⁵³ and in $\text{Nd}_2\text{Ir}_2\text{O}_7$.¹⁴

Now we come to our observation of linear specific heat in all three samples at low temperature insulating phase. This is most unusual. Linear specific heat can occur in Fermi system in weak localization regime, because of non zero density of states near the Fermi energy, but like we discussed earlier the temperature dependent resistivity rules out weak localisation. Weyl fermions show non-metallic resistivity (negative temperature coefficient of resistivity) but because of their linear dispersion, Weyl fermions would rather give a T^3 specific heat. Antiferromagnets in frustrated lattices often give spin-liquid ground states supporting exotic excitations called spinons obeying fractional quantum statistics.⁵⁴ Theoretical⁵⁵ analysis of Kagome lattice antiferromagnet suggests that, a linear specific heat in insulating antiferromagnet is possible if spinons have finite area Fermi surface. Spin liquids are like spin superfluids (pairing between spinons of opposite spins) with or without gap for spinon excitations.⁵⁶ Free spinons give linear specific heat. In $x=0.0$ material γ does not change with

the magnetic field and this is consistent with a spin liquid state having gapless spinon excitations^{42,43} coexisting with long range antiferromagnetic ordering³⁷ as is observed in other magnetically ordered systems.⁴⁹⁻⁵¹ The magnitude of γ in $x=1.0$ compound is also much larger (this is due to contribution of spinons from both the Ir and Nd sublattice) than in $x=0.0$ compound in zero field. It is also possible that Nd spin system develops spin liquid kind of singlet formation due to f-d exchange interaction. The f-d exchange interaction gets modified beyond a certain applied magnetic field which induces breaking of Nd and Ir spin singlets. Hence, in $x=1.0$, γ varies superlinearly beyond certain magnetic field and do not show any sign of saturation even at 90 kOe (see inset of fig. 8(b)). This suggests that spin liquid type singlet correlation is in both Ir and Nd spin sub-systems without affecting the long range antiferromagnetic ordering. Here we would like to point out categorically that there is coexistence of Neel order (AIAO)^{24,29} and singlet spin liquid order (i.e., long range resonating valence bond ordering).⁴⁹⁻⁵¹ It needs more experimental investigation of two pyrochlore antiferromagnets coupled by f-d exchange.

Conclusion

From different magnetic field cycling MR it is clear that these materials are fragmented into domains with larger resistivity (larger charge gap) separated by domain walls with lesser resistivity (lesser charge gap). From our analysis of magnetic susceptibility, low temperature linear specific heat and negative magnetoresistance with low field quadratic and high field linear dependence we conclude that, the magnetic state of Ir electrons in the domains (larger volume fraction), is very weak antiferromagnetic AIAO ordering superimposed on a predominantly possible chiral spin liquid state, i.e coexistence of AIAO ordering and chiral spin liquid. Observation of linear specific heat in the insulating low temperature phase rules out the possibility of Weyl semimetal phase in these materials. Linear specific heat comes from spinons, which are excitations above the spin liquid state. We also conclude that f-d exchange interaction encourages singlet correlation (spinon pairing). Transport properties like resistivity and magnetoresistance comes from the domain wall regions, where small AIAO ordering of Ir moments is destroyed, leading to smaller charge gap than in the domains. In $x=0.0$ material, this chiral spin liquid gives very small negative magnetoresistance. In $x=0.5$ and 1.0 materials magnetoresistance is hugely amplified by Kondo scattering of rare earth moments with the chiral spin liquid. Chiral spin liquid along with Kondo scattering could be exciting areas that might lead to new physics.

Acknowledgement

One of the author SM would like to thank Anish Karmahapatra, ECMP Division, SINP for XRD measure-

ments. This work is partially supported by SERB, DST, GOI under TARE project (File No.:TAR/2018/000546).

References

- ¹ O. Vafek and A. Vishanath, *Annu. Rev. Condens. Matter Phys.* 5, 83 (2014)
- ² William Witczek-Krempa, Gang Chen, Y. B. Kim and L. Balents, *Annu. Rev. Condens. Matter Phys.* 5, 57(2014), M. Z. Hasan and C. L. Kane, *Rev. Mod. Phys.* 82, 3045(2010), X. L. Qi and S. C. Zhang, *Rev. Mod. Phys.* 83, 1057 (2011).
- ³ Z. K. Liu, B. Zhou, Y. Zhang, Z. J. Wang, H. M. Weng, O. Prabhakaran, S. K. Mo, Z. X. Shen, Z. Fang, X. Dai, Z. Hussain and Y. L. Chen, *Science* 343, 864 (2014), M. Neupane, Su-Yang Xu, R. Sankar, N. Alidoust, Guang Bian, Chang Liu, I. Belopolski, Tay-Rong Chang, Horng-Tay Jeng, Hsin Lin, Arun Bansil, Fangcheng Chou and M. Zahid Hasan, *Nat. Commun.* 5, 3786 (2014), Su-Yang Xu, Chang Liu, I. Belopolsky, S. K. Kushwaha, R. Sankar, J. W. Krizan, T. R. Chang, C. M. Polley, J. Adell, T. Balasubramanian, K. Miyamoto, N. Alidoust, Guang Bian, M. Neupane, H-T. Jeng, C-Y, Huang, W-F. Tsai, T. Okuda, A. Bansil, F. C. Chou, R. J. Cava, H. Lin and M. Z. Hasan, *Phys. Rev. B* 92, 075115 (2015), S. Borisenko, Wuinn Gibson, Danil Evtushinsky, V. Zabolotnyy, B. Buchner and R. J. Cava, *Phys. Rev. Lett.* 113, 027603 (2014).
- ⁴ B. Q. Lv, N. Xu, H. M. Weng, J. Z. Ma, P. Richard, X. C. Huang, L. X. Zhao, G. F. Chen, C. E. Matt, F. Bisti, V. N. Strocov, J. Mesot, Z. Fang, X. Dai, T. Qian, M. Shi and H. Ding, *Nat. Phys.* 11, 724 (2015), S-Y. Xu et al, *Nat. Phys.* 11, 748 (2015).
- ⁵ X. Wan, A. M. Turner, A. Vishwanath, and S. Savrasov, *Phys. Rev. B* 83, 205101 (2011),
- ⁶ Takumi Ohtsukia, Zhaoming Tiana, Akira Endoa, Mario Halima, Shingo Katsumotoa, Yoshimitsu Kohamaa, Koichi Kindoa, Mikk Lippmaaa, and Satoru Nakatsujia, *PNAS*, 116, 8803 (2019).
- ⁷ D. T. Son and B. Z. Spivak, *Phys. Rev. B* 88, 104412 (2013).
- ⁸ Yo Machida, Satoru Nakatsuji, Shigeki Onoda, Takashi Tayama and Toshiro Sakakibara, *Nature*, 463 (2010).
- ⁹ D. Pesin and L. Balents, *Nat. Phys.* 6, 376(2010).
- ¹⁰ S. Nakatsuji, Y. Machida, Y. Maeno, T. Tayama, T. Sakakibara, J. van Duijn, L. Balicas, J. N. Millican, R. T. Macaluso and Julia Y. Chan, *Phys. Rev. Letters*, 96, 087204 (2006).
- ¹¹ B. J. Kim, H. Ohsumi, T. Komesu, S. Sakai, T. Morita, H. Takagi and T. Arima, *Science* 323, 1329 (2009), Y-Z. You, I. Kimchi and A. Vishwanath, *Phys. Rev. B* 86, 085145 (2012).
- ¹² Hongbin Zhang, Kristjan Haule, and David Vanderbilt, *Phys. Rev. Letters*, 118, 026404 (2017).
- ¹³ Daiki Yanagishima, Yoshiteru Maeno, *Journal of the Physical Society of Japan*, 70, 2880 (2001).
- ¹⁴ Kazuyuki Matsuhira, Makoto Wakeshima, Yukio Hinatsu, Seishi Takagi, *Journal of the Physical Society of Japan*, 80, 094701 (2011).
- ¹⁵ Jun. J. Ishikawa et al, *Phys. Rev. B* 85, 285109 (2012).
- ¹⁶ A. B. Sushkov, J. B. Hofmann, G. S. Jenkins, J. Ishikawa, S. Nakatsuji, S. Das Sarma and H. D. Drew, *Phys. Rev. B* 92, 241108(R) (2015).
- ¹⁷ F. F. Tafti, J. J. Ishikawa, A. McCollam, S. Nakatsuji and S. R. Julian, *Phys. Rev. B* 85, 205104 (2012).
- ¹⁸ G. Chen and M. Hermele, *Phys. Rev. B*, 86, 235129 (2012).
- ¹⁹ Kazuyuki Matsuhira, Asashi Tokunaga, Makoto Wakeshima, Yukio Hinatsu, and Seishi Takagi, *Journal of the Physical Society of Japan* 82, 023706 (2013).
- ²⁰ T. Hasegawa, N. Ogita, K. Matsuhira, S. Takagi, M. Wakeshima, Y. Hinatsu and M. Udagawa, *Journal of Physics: Conference Series* 200 012054 (2010).
- ²¹ K. Ueda, J. Fujioka, Y. Takahashi, T. Suzuki, S. Ishiwata, Y. Taguchi, and Y. Tokura, *Phys. Rev. Letters*. 109, 136402 (2012).
- ²² Zhaoming Tian, Yoshimitsu Kohama, Takahiro Tomita, Hiroaki Ishizuka, Timothy H. Hsieh, Jun J. Ishikawa, Koichi Kindo, Leon Balents and Satoru Nakatsuji, *Nature Physics*, 134 2016.
- ²³ M. Nakayama, T. Kondo, Z. Tian, J. J. Ishikawa, M. Halim, C. Bareille, W. Malaeb, K. Kuroda, T. Tomita, S. Ideta, K. Tanaka, M. Matsunami, S. Kimura, N. Inami, K. Ono, H. Kumigashira, L. Balents, S. Nakatsuji and S. Shin, *Phys. Rev. Letters*. 117, 056403 (2016).
- ²⁴ H. Guo, C. Ritter and A. C. Komarek, *Phys. Rev. B* 94 161102(R) (2016).
- ²⁵ K. Tomiyasu, K. Matsuhira, K. Iwasa, M. Watahiki, S. Takagi and M. Wakeshima, *Jour. Phys. Soc. Japan*, 81, 034709 (2012).
- ²⁶ K. Ueda, J. Fujioka, B.-J. Yang, J. Shiogai, A. Tsukazaki, S. Nakamura, S. Awaji, N. Nagaosa and Y. Tokura, *Phys. Rev. Letters*, 115, 056402 (2015).
- ²⁷ H-J Koo, M. H. Whangbo and B. J. Kennedy, *Jour. Solid. State. Chem*, 136, 269 (1998).
- ²⁸ S Zhao, J. M. Mackie, D. E. MacLaughlin, O. O. Bernal, J. J. Ishikawa, Y. Ohta, and N. Nakatsuji, *Phys. Rev B* 83, 180402 (2011).
- ²⁹ S. M. Dissele, C. Dhital, T. C. Hogan, A. Amato, S. R. Giblin, C. de la Cruz, A. D. Aladine, S. D. Wilson and M. J. Graf, *Phys. Rev B* 85, 174441 (2012), H. Guo, K. Matsuhira, I. Kawasaki, M. Wakeshima, Y. Hinatsu, I. Watanabe and Zhu-an Xu, *Phys. Rev. B* 88, 060411(R) (2013).
- ³⁰ W. Witczak-Krempa and Yong Baek Kim, *Phys. Rev B* 85, 045124 (2012).
- ³¹ Prachi Telang, Kshiti Mishra, A. K. Sood and Surjeet Singh, *Phys. Rev. B* 97, 235118 (2018).
- ³² A. Banerjee, J. Sannigrahi, S. Giri, S. Majumdar, *Phys. Rev. B* 96, 224426 (2017).
- ³³ Z. Porter, E. Zoghlin, S. Britner, S. Husremovic, J. P. C. Ruff, Y. Choi, D. Haskel, G. Laurita and S. D. Wilson, *Phys. Rev. B* 100, 054409 (2019).
- ³⁴ Eric Yue Ma, Y. T. Cui, K. Ueda, S. Tang, K. Chen, N. Tamura, P. M. Wu, J. Fujioka, Y. Tokura and Zhi-Xun Shen, *Science* Vol 350, 538 (2015).
- ³⁵ Hai-Zhou Lu and Shun-Qing Shen, *Phys. Rev. B* 92, 035203 (2015).
- ³⁶ A. Malinowska, M.Z. Cieplaka, M. Berkowska and S. Guha: *Proceedings of the XI National School Collective Phenomena and Their Competition* Kazimierz Dolny,

- September 25-29, 2005. N. Mott, *Conduction in Non-Crystalline Materials* (Clarendon, Oxford, 1993).
- ³⁷ Sagayama H, Uematsu D, Arima T, K. Sigimoto, J. J. Ishikawa, E. O'Farrell, and S. Nakamatsu, *Phys. Rev. B* 87,100403(R) (2013).
- ³⁸ Yusuke Takikawa, Shuji Ebisu, Shoichi Nagata, *Journal of Physics and Chemistry of Solids*, 71, 1592 (2010).
- ³⁹ A. Bertin, P. D. de Reotier, B. Fak, C. Martin, A. Yaouanc, A. Forget, D. Sheptyakov, B. Frick, C. Ritter, A. Amato, C. Baines and P. J. C. King, *arXiv.org : cond-mat/1511.00987*, Nov 2015 .
- ⁴⁰ N. Ghosh, U. K. Roßler, K. Nenkov, C. Hucho, H. L. Bhat and K-H. Muller, *J. Phys.: Condens. Matter* 20, 395219 (2008).
- ⁴¹ M. Watahiki, K. Tomiyasu, K. Matsuhira, K. Iwasa, M. Yokoyama, S. Takagi, M. Wakeshima and Y. Hinatsu, *Journal of Physics: Conference Series* 320, 012080 (2011).
- ⁴² S. Yamashita, Y. Nakazawa, M. Oguni, Y. Oshima, H. Nojiri, Y. Shimizu, K. Miyagawa, and K. Kanoda, *Nat. Phys.* 4, 459 (2008).
- ⁴³ S. Yamashita, T. Yamamoto, Y. Nakazawa, M. Tamura, and R. Kato, *Nat. Comms.* 2, 275 (2011).
- ⁴⁴ T. C. Fujita, Y. Kozuma, M. Uchida, A. Tsukazaki, T. Arima and M. Kawasaki, *Scientific Reports, Nature* 5, 9711 (2015).
- ⁴⁵ X. G. Wen, Krank Wilczek and A. Zee, *Phys. Rev. B* 39, 11413 (1989).
- ⁴⁶ N. Nagaosa, X. Z. Yu and Y. Tokura, *Gauge fields in real and momentum space in magnets : monopoles and skyrmions*, *Pilos. Trans. A. Math. Phys. Engg. Sci* 370, 5806 (2012).
- ⁴⁷ Y. Taguchi, Y. Oohara, H. Yoshizawa, N. Nagaosa and Y. Tokura, *Science* 291, 2573 (2001).
- ⁴⁸ A. Neubauer, C. Pfleiderer, B. Binz, A. Rosch, R. Ritz, P. G. Niklowitz, and P. Boni, *Phys. Rev. Letters*, 102, 186602 (2009).
- ⁴⁹ T. Nagata, H. Fujino, K. Ohishi, J. Akimitsu, S. Katano, M. Nishi, K. Kakurai, *Journal of Physics and Chemistry of solids* 60, 1039 (1999).
- ⁵⁰ A. Zorko, M. Pregelj, M. Klanjšek, M. Gomilšek, Z. Jagličič, J. S. Lord, J. A. T. Verezhak, T. Shang, W. Sun and J.-X. Mi, *Phys. Rev. B* 99, 214441 (2019).
- ⁵¹ Eric M. Kenney, Carlo U. Segre, William Lafargue-Dit-Hauret, Oleg I. Lebedev, Mykola Abramchuk, Adam Berlie, Stephen P. Cottrell, Gediminas Simutis, Faranak Bahrami, Natalia E. Mordvinova, Gilberto Fabbris, Jessica L. McChesney, Daniel Haskel, Xavier Rocquefelte, Michael J. Graf and Fazel Tafti, *Phys. Rev. B* 100, 094418 (2019).
- ⁵² A. C. Hewson, *The Kondo problems of Heavy Fermions* , Cambridge Univ. Press(Cambridge, England) 1993.
- ⁵³ L. Balicas, S. Nakatsuji, Y. Machida and S. Onoda, *arXiv.org : cond-mat /1105.2986*, May 2011. N. Harrison, D. G. Nocera, Y. Takano and Y. S. Lee, *arXiv.org : cond-mat/ 1402.2693*, February 2014.
- ⁵⁴ L. Balents, *Nature* 464, 199 (2010).
- ⁵⁵ Ying Ran, M. Hermele, Patrick. A. Lee and X. G. Wen, *Phys. Rev. Letters.* 98, 117205 (2007).
- ⁵⁶ G. Baskaran, Z. Zou and P. W. Anderson, *Solid. State, Commun. Vol* 63, No. 11 , 973 (1987).